Al-Nahrain Journal of Science
ANJS, Vol. 27 (2), June, 2024, pp. 81-87

# Modified Satellite Image Segmentation Based on Region Method

Ali Jassam Mohammed*, Laith A. Al-Ani

Department of Physics, College of Science, Al-Nahrain University, Jadiriya 64055, Baghdad Iraq.

**Article's Information**

Received: 04.01.2024
Accepted: 24.01.2024
Published:15.09.2024

**Keywords:**
Image segmentation
Principal Component Analysis
Region based method
Chain coding

**Abstract**

A modified segmentation technique is proposed to segment images using Univariate statistical parameters such as minimum, maximum, and mean values as well as contour length. This segmentation technique is applied to satellite images of seven bands captured by the Landsat (8, 9) OLI satellite in 2022. The utilization of principal component analysis (PCA) is employed in this study, as it has been observed that the combined value of the initial three principal components encompasses nearly 99% of the pertinent information. To effectively represent the identified elements, the Freeman chain coding technique is applied, ensuring both reduced bounds and low bit rates. The segmentation process for the 1st PC images involves several stages. This approach employs a threshold value of 0.60 and a minimum contour length of 8. The process commences at the initial stage and advances consistently until it reaches the final stage, ultimately generating an image devoid of any fragmented regions. The suggested segmentation method provides realistic thin and closed borders compared to any method based on the edge-based technique. The results showed that the total number of segment regions with a contour length greater than 6 equals 358 within four categories that have the same characteristic.

http://doi.org/10.22401/ANJS.27.3.10
*Corresponding author: alijm1747@gmail.com


## 1. Introduction

Image segmentation is a commonly utilized technique that seeks to divide an image into separate and significant segments, each possessing similar attributes and characteristics. Image segmentation is a critical and intricate phase in the field of image processing, presenting notable difficulties. Its objective is to partition an image into separate and significant regions, utilizing distinct characteristics like color, texture, or shape. This technique holds immense importance in computer vision and image processing, as it facilitates the detection and isolation of various objects or regions within an image [1,2]. Image processing is utilized in a multitude of ways, encompassing content-based image retrieval, machine vision, medical imaging, object detection, video surveillance, recognition tasks, and joint object segmentation. Another emerging domain within this field is remote sensing, which involves the detection and analysis of data collected from the Earth's surface using remote sensors. These sensors effectively capture and quantify the energy reflected by the ground, thereby offering valuable insights for various applications. Satellites serve as a prominent illustration of remote sensing technology [3]. The primary objective of the segmentation process is to acquire additional data from a particular region within an image and simplify the process of labeling the object scene. There are three distinct categories of image segmentation techniques, which are determined by the characteristics of the image: edge-based segmentation methods, region-based segmentation methods, and threshold segmentation methods [4, 5]. Thresholding is a popular technique for image segmentation, where a threshold value is used to separate pixels in an image into two groups based on their intensity values. This approach uses image

discontinuity segmentation to recognize lines, edges, and isolated points when there are sudden changes in local attributes. The partition result is then generated by inferring the borders of the areas. The uniformity of spatially dense information, such as texture, intensity, and color, is utilized by the second technique. The third method combines boundary-based image segmentation with region-based image segmentation [6-11]. The primary objective of this research is to partition multispectral satellite images obtained from the Thematic Mapper (TM). To accomplish this, the Principal Component Analysis (PCA) technique will be employed on the initial bands. The resultant image will comprise the first three components, which will encompass the majority of the pertinent information. This methodology represents an unsupervised classification approach. PCA endeavors to amalgamate and streamline information from multiple input images into a reduced set of principal component images. This transformation entails converting a collection of interconnected variables from the input domains into uncorrelated variables within the PC output domain. The assessment of materiality also holds significance within this procedure.

## 2. Study Area

The images were taken by the Landsat (8, 9) OLI satellite in 2022. The scene consists of seven bands with a resolution of 512 x 512. ENVI software was utilized to perform atmospheric and geometric corrections on all the satellite image bands.
Figure (1-a) represents the images of TM bands, the x-axis is the column, the z-axis is the row index, and the y-axis is the band number or wavelength of a given band while Figure (1-b) represents the stretched image of the Band 7.

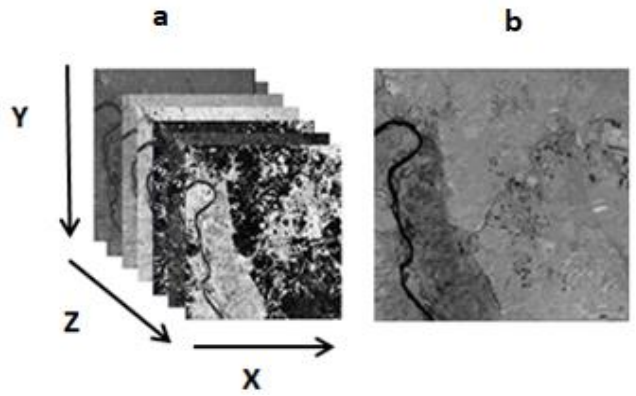


**Figure 1.** (a) Multispectral image bands, (b) Stretched image of band 7.

The presented scene is of the Nimrud sub-district of Al-Hamdaniya district, which is about 30 kilometers away from the center of Mosul Governorate. The city of Nimrud is one of the regions located in the south of Mosul Governorate in Iraq. It is characterized by environmental diversity, as it is located on the side of the Tigris River, which is the main source of water. The Nimrud area consists of vast agricultural lands. It also contains orchards and farms, in addition to residential areas, archaeological areas, and water regions.

## 3. Methodology

The methodology of this work will be explained thoroughly, beginning with the use of principal component analysis, and concluding with the implementation of the suggested segmentation method.

### 3.1. Mathematical description of PCA

Suppose that the satellite image consists of several bands, with each band represented by a one-dimensional vector $x_i$ consisting of N elements. These bands are then combined into a uniform matrix ($\boldsymbol{X}$), as shown in Equation (1) [12].

$$\boldsymbol{X} = \begin{bmatrix} x_{i1} \\ x_{i2} \\ x_{i3} \\ x_{1N} \end{bmatrix} \quad \dots (1)$$

where, $x_{ij}$ is the j[th] component of the vector $\boldsymbol{X}$. The mean of the vector can be determined by the average given by [12]

$$\mathbf{m_x} = \mathbf{E\{X\}} \quad \dots (2)$$

To ensure that the 1st PC aligns with the direction of maximum contrast, mean centering is performed. The covariance matrix $\sum_{\mathbf{x}}$ (A measure of the degree of association between two variables) of the mean centering vector x, which comprises N components, can be represented as [13]:

$$\sum_{\mathbf{x}} = \mathbf{E}\{(\mathbf{X} - \mathbf{m_x})(\mathbf{X} - \mathbf{m_x})^{\mathbf{T}}\} \quad \dots (3)$$

where $\mathbf{E}$ is the expected value), T: indicates transposition. The eigenvalues of the covariance matrix $\sum_{\mathbf{x}}$ play an essential role in calculating the covariance matrix of the transformed data $\sum_{\mathbf{y}}$. This important connection is obtained as [13]:

$$\sum_{\mathrm{y}} = \mathrm{A}\sum_{x}\mathrm{A}^{T} = \begin{pmatrix} \lambda_1 & 0 & \cdots & 0 \\ 0 & \lambda_2 & 0 & 0 \\ \vdots & 0 & \ddots & 0 \\ 0 & 0 & 0 & \lambda_N \end{pmatrix} \quad \dots (4)$$

where A represents the constructed eigenvectors matrix which is defined by the following equation

$$A = \begin{pmatrix} e_{1,1} & \cdots & e_{1N} \\ \vdots & \ddots & \vdots \\ e_{N1} & \cdots & e_{NN} \end{pmatrix} \quad \dots (5)$$

In this particular situation, $\lambda_i$ represents the eigenvalues $(i = 1, 2, \dots, N)$ associated with the eigenvector $e_i$ of the covariance matrix $\sum_x$.

### 3.2. Region based methods

The literature divides region-based segmentation approaches into three types [14, 15]; region merging, region splitting, and a combination of both splitting and merging. These methods generate higher level primitives unless the image contrast is extremely low. The faint objects or regions are merged with the image background in this case [3, 16]. The region merging method is a technique based on merging regions of similar density separated by weak boundaries into larger regions, while the region division process is carried out by separating the image into groups of regions based on the threshold value taken from the image histogram. Each of these regions has a consistent characteristic, such as color or texture. Cohesive or homogenous are terms used to describe these regions. The segmentation procedure begins with the entire image and works its way through the collection of homogeneous regions. Homogeneous regions are not usually relevant and are only desirable when searching for subclasses of regions [17, 18]. It is worth to mention that region-based methods are very effective on multispectral images. These methods produce higher level primitives but most of the time; these regions do not correspond to physical entities unless their intensity differs everywhere from the background. For multispectral images, region-based techniques are particularly successful. These techniques produce higher-level primitives, even though these areas are typically not linked to concrete physical entities until their intensity significantly deviates from the surrounding background [15]. As mentioned earlier, the objective of image segmentation is to partition an image into distinct regions. Let R represent the entire region of the image. Segmentation can be viewed as a process that divides R into n sub regions, namely $R_1, R_2, R_3, \dots, R_n$ and each of these sub regions is then analyzed based on the criteria outlined in [19]:

1. $\bigcup_{i=1}^{n} R_i = R$
2. $As\ R_i\ is\ connected\ region, i = 1, 2, \dots, n$
3. $R_i \cap R_j = \phi \quad for\ all\ i\ and\ j, i \neq j$
4. $P(R_i) = True \quad for\ i = 1, 2, \dots n$
5. $P(R_i \cup R_j) = False \quad for\ i \neq j$

In this study, the approach of division employed will be outlined as follows: The logical predicate $P(R_i)$ is defined over the points in set $R_i$, while $\phi$ represents the empty set. The 1st requirement requires that the segmentation is complete, meaning that every pixel must be assigned to a region. The 2nd requirement states that the points within a region must be connected. The 3rd requirement emphasizes the need for the regions to be split. The 4th requirement is based on the verification of the pixels within a segmented region are required to satisfy. Finally, the 5th requirement states that the regions $R_i$ and $R_j$ must be distinct based on the predicate P.

### 3.3. Chain coding

Freeman invented the chain coding technique, which has been utilized for pattern detection and data compression. This technique represents the boundary points as a string using freeman's direction codes. Codes of four or eight directions can be used, but the eight-direction codes are more common [20, 21]. In this study, the Freeman chain code approach with an 8-direction code is used to find contours, as illustrated in fig (2), since it is obvious that for a rectangular grid, if a point on a continuous curve is known, the next point can only occupy one of eight potential adjacent positions.


**Figure 2.** Eight possible directions of the chain code

### 3.4. Region segmentation using split technique

The selection of the appropriate threshold value is one of the key factors in separating the object from its background. In this study, the threshold value was chosen based on the Univariate statistics of the scene such as the minimum (Min), maximum (Max), and average value (Mean) of the histogram. The modified algorithm divides the region into parts and defines its outer boundaries as in the following algorithm:

i. The values Min, Max, and Mean for the histogram are calculated for the whole image, and then the next parameter F is calculated according to the following relation

$$F = \frac{\left((Max. - Min.)\right)}{2} \quad \ldots (6)$$

ii. For each pixel in the image the following condition will be applied

$$|Pixel\ Value - Mean| \leq F \quad \ldots (7)$$

If the previous condition is true, give the pixel a particular value, such as the number 1 (indicating a certain color), to symbolize the area of the first segment region. The pixel will be given a different color, such as the number 2, which indicates the remaining portion of the image, if the aforementioned criterion is not satisfied.

iii. Repeat steps 1 and 2 for the residual image until

$$F < |Pixel\ value - Mean| \quad \ldots (8)$$

The scene is formed of various colored sections at the conclusion of this process. We consider that areas with the same color share common characteristics and belong to the same class.

iv. Create an empty matrix to move regions of the same color.

v. Each isolated image point is designated as an edge point if the absolute values of its vertical and horizontal neighbors differ. By the completion of this stage, only the borders of each separate area will be indicated with the identical color to symbolize the distinct region. The requirement to transmit and store digital images with minimal data usage in various applications has prompted us to employ Chain Encoding, one of the most commonly utilized error-free encoding methods.

vi. Repeat step 4 and 5 for all colored region in the scene.

## 4. Experiment Results and Discussion

Table 1 displays the Univariate statistical variables' minimum (Min), maximum (Max), and mean values for the seven bands.

**Table 1.** Univariate Statistical Variables for Seven input Spectral Bands.

| Band | Min | Max | Mean |
|---|---|---|---|
| 1 | 23 | 408 | 90.04 |
| 2 | 15 | 401 | 94.25 |
| 3 | 18 | 512 | 147.9 |
| 4 | 18 | 520 | 194.4 |
| 5 | 17 | 555 | 275.2 |
| 6 | 23 | 548 | 297.3 |
| 7 | 21 | 439 | 233.1 |

The Covariance variance matrixes of the spectral bands for seven bands are shown in the table 2.

**Table 2.** Covariance variance matrixes of the input spectral bands

| Band | 1 | 2 | 3 | 4 | 5 | 6 | 7 |
|---|---|---|---|---|---|---|---|
| 1 | 252.1 | 292.3 | 419.9 | 596.9 | 238.9 | 696.0 | 686.3 |
| 2 | | 348.4 | 509.8 | 739.1 | 326.6 | 868.7 | 839.5 |
| 3 | | | 784.4 | 1160.0 | 606.6 | 1392.7 | 1321.2 |
| 4 | | | | 1782.5 | 902.1 | 2157.6 | 2045.7 |
| 5 | | | | | 1794.8 | 1477.1 | 992.2 |
| 6 | | | | | | 2944.7 | 2671.0 |
| 7 | | | | | | | 2595.3 |

The result of the first three Eigenvalues and Eigenvectors are tabulated in Tables 3 and 4, respectively.

**Table 3.** The 1st three eigenvalues ($\lambda_i$) computed from the covariance matrix

| $\lambda_1$ | $\lambda_2$ | $\lambda_3$ |
|---|---|---|
| 0.85 | 0.12 | 2.2E-02 |

It can be observed from table 3 of eigenvalues and the amount of variance for each principal component that the cumulative value of the first three principal components contains almost 99% of the information. However, there is no meaningful data on the remaining principal components (PCs).

**Table 4.** The 1st three eigenvector ($e_i$) computed from the covariance matrix

| $e_1$ | $e_2$ | $e_3$ |
|---|---|---|
| 0.145 | -0.117 | 0.365 |
| 0.179 | -0.116 | 0.398 |
| 0.284 | -0.105 | 0.456 |
| 0.434 | -0.174 | 0.381 |
| 0.283 | 0.923 | 0.115 |
| 0.569 | -0.047 | -0.407 |
| 0.523 | -0.277 | -0.420 |

By applying principal component analysis (PCA) to the seven-band images, we obtain a set of seven principal component images. Figure 3 illustrates the three primary main components.


**Figure 3.** The first three principal component images.

Figure 4 illustrates the various stages involved in the segmentation process of the proposed method for the 1st PC images. This approach utilizes a threshold value of 0.60 and a minimum contour length of 8. The procedure initiates from the initial stage and progresses steadily until it reaches its final phase, ultimately resulting in an image that is free from any segmented regions. This figure show that The 1st PC satellite image, which is initially positioned at the top right. On the other hand, the following images (b to e) illustrate the resultant images achieved from the segmentation process at each step (loop) of the program's execution, depending on the selected Univariate statistics.

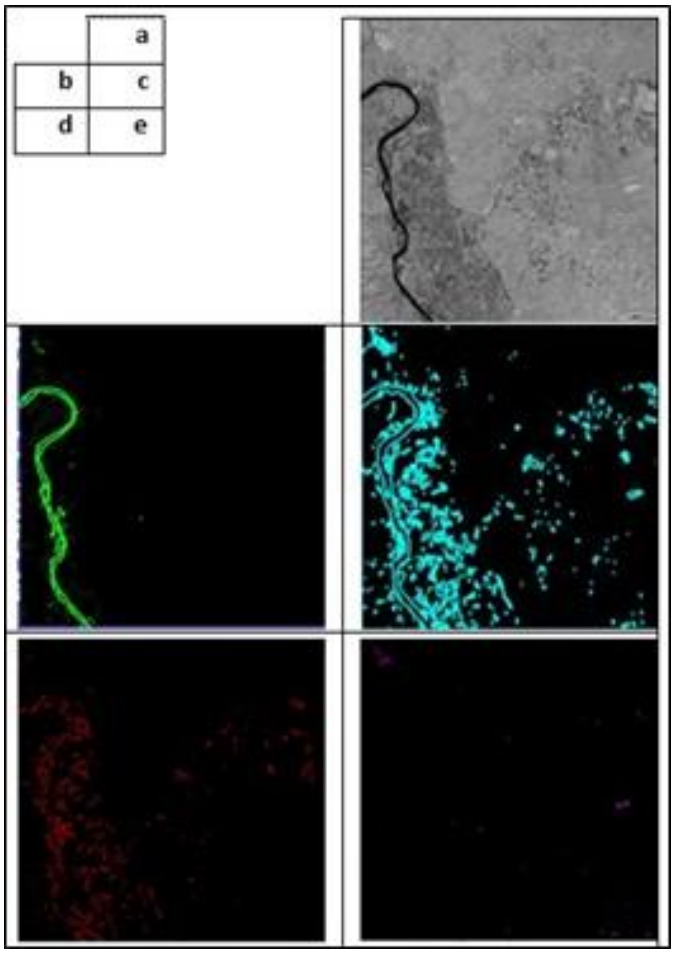


**Figure 4.** The boundaries of each segmented region for 1st PC image.

Table 1 presents a visual representation of the number of segmented regions that possess enclosed boundaries at various stages of program execution.

Table 1. The nnumber of segmented regions at various stages of program execution.

| | Threshold = 0.6<br>Length of Adopted Chain = 8 | |
|---|---|---|
| | Number of colosed regions | |
| Loop Number | Each loop | Final results |
| 1 | 3 | 358 |
| 2 | 213 | |
| 3 | 134 | |
| 4 | 8 | |

At the end of this procedure, boundaries of different regions will be marked with different colors referring to different classes, see fig 5, In fact color assigned to boundaries are used to classify different regions.

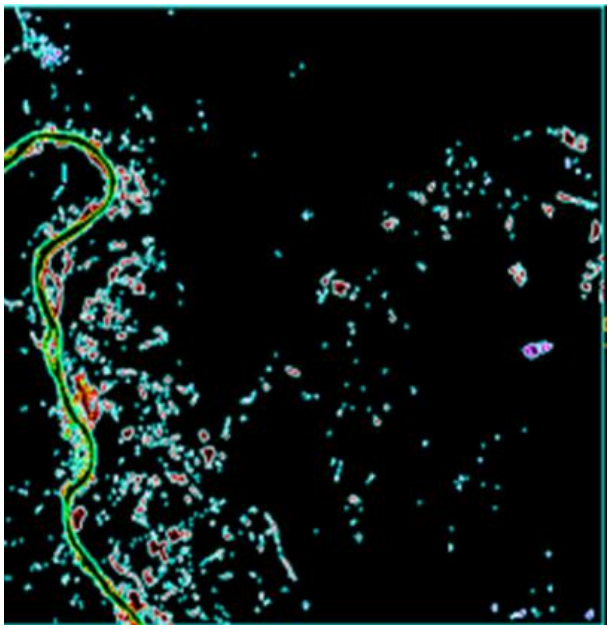

**Figure 5.** The result of the suggested segmentation algorithm for the 1st PC image.

## 5. Conclusions

It should be emphasized that the quantity of closed contour cutting spaces per loop number is contingent upon the initial determination of the contour length. In this investigation, the minimum contour length employed was 8. The findings indicate that within the four categories sharing the same characteristic (number of loops), there exist 358 segment regions with a cumulative contour length exceeding 8. To summarize, the region-based approach utilized in this study yields a closed contour for the segmented region with clearly defined boundaries, surpassing any technique reliant on the edge-based approach. Additionally, this adopted technique facilitates the classification of each segmented region. In this study, the space image segmentation process was enhanced by implementing the suggested segmentation method with the principal components analysis technique. Moreover, the proposed segmentation method exhibits the potential to be applied to both monochromatic and polychromatic images, including medical images.

**Funding:** This research is self-funded

**Conflict of Interest:** The authors declare no conflict of interest.

## References

[1] Kaur, M.; Chand, L.; "Review of image segmentation and its techniques". J. Emer. Technol. Innov. Res. 5(7): 974-981, 2018.
[2] Kaur, D.; Kaur, Y.; "Various image segmentation techniques: a review". Int. J. Comp. Sci. Mob. Comp. 3(5): 809-814, 2014.
[3] Sonali, S.S.; Ulhas P.; Ajay, K.; "image segmentation technique: a systematic literature review". Int. J. Eng. Res. Technol. 12(01): 180-185, 2023.
[4] Houssein, E.H. et al.; "An improved tunicate swarm algorithm for global optimization and image segmentation". IEEE Access 9: 56066-56092, 2021..
[5] Al-Ani, L.A.; "Classification of Digital Satellite Images". Ph. D .Thesis. 1996, Al-Nahrain University.
[6] Al-Amri, S.S.; Kalyankar, N.; Khamitkar, S.; "Image segmentation by using edge detection". Int. J. Comp. Sci. Eng. 2(3): 804-807, 2010.
[7] Tobias, O.J.; Seara, R.; "Image segmentation by histogram thresholding using fuzzy sets". IEEE Trans. Image Proc. 11(12): 1457-1465, 2002.
[8] Pal, N.R.; Pal, S.K.; "A review on image segmentation techniques". Patt. Recog. 26(9): 1277-1294, 1993.
[9] Gonzalez, R.; Woods, R.; "Digital image processing" 2017, New York: John Wiley and Sons.
[10] Abdulateef, S.K.; Salman, M.D.; "A Comprehensive Review of Image Segmentation Techniques". Iraqi J. Elect. Elect. Eng. 17(2), 2021.
[11] Zaitoun, N.M.; Aqel, M.J.; "Survey on image segmentation techniques". Proc. Comp. Sci. 65: 797-806, 2015.
[12] Laith, A.A.; Ayad, A.A.; Alyaa, H.A.; "Principal Component Analysis of Multi-Temporal Image Pairs". Iraqi J. Sci. 47(1): 220-226, 2006.
[13] Abdulmajeed, M.A.; Laith A.A.; "Estimation of Wheat Yield on a Farm in Najaf/Iraq, using Principal Component Analysis of Multi Temporal Satellite Images Pairs". IOP Conference Series: Earth and Environmental Science. 1202(1). IOP Publishing, 2023.
[14] Angelina, S.; Suresh, L.P.; Veni, S.K.; "Image segmentation based on genetic algorithm for region growth and region merging". International conference

on computing, electronics and electrical technologies (ICCEET). 2012.
[15] King, M.; Zhu, B.; Tang, S.; "Optimal path planning". Mobile Robots 8(2): 520-531, 2001.
[16] Simpson, H.; Dumb R.; 3rd ed., Springfield: UOS Press, 2004, pp.6-9.
[17] King, v; Zhu, B.; "Gaming strategies". Path Planning to the West, II(S). Tang and M. King, Eds. Xian: Jiaoda Press, 1998, pp. 158-176.
[18] Simpson, B. et al. "Title of paper goes here if known," unpublished, 2020.
[19] Lu, J. G.; "Title of paper with only the first word capitalized". J. Name Stand. Abbrev., 2022.
[20] Yorozu, Y.; Hirano, M.; Oka, K.; Tagawa, Y.; "Electron spectroscopy studies on magneto-optical media and plastic substrate interface". Digest 9th Annual Conf. Magnetics Japan, August 1987.
[21] Young, v; The Technical Writer's Handbook, Mill Valley, CA: University Science, 1989.